The reactivity of 2,2′-bipyridine complexes in the electrochemical reduction of organohalides

D. G. Yakhvarov,[a] E. G. Samieva,[a] D. I. Tazeev,[a,b] and Yu. G. Budnikova[a,b]★

[a]A. E. Arbuzov Institute of Organic and Physical Chemistry, Kazan′ Research Center, Russian Academy of Sciences, 8 ul. Akad. Arbuzova, 420088 Kazan′, Russian Federation. Fax: +7 (843 2) 75 2253. E-mail: yulia@iopc.knc.ru
[b]Kazan′ State University, 18 ul. Kremlyovskaya, 420008 Kazan′, Russian Federation. Fax: +7 (843 2) 31 5416

Nickel(0) complexes coordinatively unsaturated with 2,2′-bipyridine (bpy) are more reactive in the oxidative addition to organic halides than the saturated analogs. σ-Organonickel complexes formed as intermediates of catalytic cycles were prepared in high yields using nickel complexes coordinatively unsaturated with bpy and aromatic halides containing a methyl group in the *ortho*-position of the ring.

Key words: nickel, 2,2′-bipyridine, alkyl halides, aryl halides, nickel, complexes, electroreduction, catalysis.

The nature of the key steps involved in the reduction of organic halides (RX) in the presence of electrochemically generated complexes of transition metals in low oxidation states,[1] in particular, Ni complexes with 2,2′-bipyridine (bpy) is little studied. It appears pertinent to study in detail the pathways of transformation of organic halides and to elucidate the nature of intermediates formed in these reactions.

The purpose of this work is to investigate the reactivity of nickel complexes containing nickel in low oxidation states and different numbers of bpy ligands in the electroreduction (ER) of RX, to elucidate more precisely the mechanism of the catalytic process, and to identify the nature of the intermediates. In order to determine the potentials of catalytic regeneration of nickel complexes in the presence of RX and the reduction potentials for the products of oxidative addition of RX to Ni^0 complexes and to estimate the reactivity of Ni^0bpy_n complexes (n = 1, 2) with respect to various substrates and the stability of intermediates formed in the catalytic cycle, we studied the electrochemical behavior of $Nibpy_nX_2$ complexes (n = 1, 3; X = Br, BF_4) in the presence of various RX (R = Pr^i, Am^i, Ph, Tol, Mes; X = I, Br).

Experimental

When recording the cyclic voltammetry (CV) curves, a stationary glass-carbon (GC) disc electrode with a working surface area of 3.14 mm^2 was used as the working electrode. The CV curves were recorded using a PI-50-1 potentiostat with a PR-49 programming unit with an electrochemical cell included in a three-electrode circuit. An XY-recorder was used; the rate of linear potential sweep was 50 mV s^{-1}. The CV curves were recorded in DMF using Et_4NBF_4 (0.1 mol L^{-1}) as the supporting electrolyte. The Ag/0.01 *M* $AgNO_3$ system in MeCN was used as the reference electrode. A Pt wire 1 mm in diameter was the auxiliary electrode. The measurements were carried out in a cell maintained at a constant temperature (25 °C) under argon. Alkyl or aryl halide RX was added to a solution of the nickel complex ($1 \cdot 10^{-2}$ mol L^{-1}) with a 10-μL chromatographic syringe.

Electrolysis was carried out using a B5-49 dc source in a 40-mL three-electrode cell in DMF solution with Et_4NBF_4 or Et_4NBr as the supporting electrolyte. The working electrode potential was checked by a Shch 50-1 dc voltmeter *vs.* the Ag/0.01 *M* $AgNO_3$ reference electrode in MeCN. The working surface area of the cylindrical Pt cathode was 20.0 cm^2. In experiments with a divided cell, tracing paper was used as the diaphragm, a GC plate with a working surface area of 4 cm^2 served as the anode, and a saturated DMF solution of the supporting electrolyte used in the catholyte served as the anolyte. In electrolysis in an undivided cell, Zn, Al, or Mg rods were employed as anodes. Prior to electrolysis, the working surface of the electrodes was conditions by grinding with emery paper. During electrolysis, the electrolyte was stirred with a magnetic stirrer and a argon continuous stream was passed through the cell.

^{1}H NMR spectra were recorded on a Varian T-60 instrument (60 MHz) in $CDCl_3$ with Me_4Si as the internal standard. The ESR signals were recorded on an SE/X-2544 Radiopan electronic spectrometer using diphenylpycrylhydrazyl (DPPH, g = 2.0036) as the internal standard. GLC analyses of reac-

Published in Russian in *Izvestiya Akademii Nauk. Seriya Khimicheskaya,* No. 5, pp. 734—741, May, 2002.

1066-5285/02/5105-796 $27.00

tion mixtures and prepared compounds were carried out on a Chrom-5 chromatograph (Czechoslovakia), using helium as the carrier gas, a heat conductivity detector, a 120×0.3 cm glass column, and 5% SE-30 on Chromaton N-AW (0.125—0.160 mm).

The MeCN solvent was purified by three fractional distillations over P_2O_5 with the addition of potassium permanganate. The concentration of the residual water was $1.8 \cdot 10^{-3}$%. DMF was purified by threefold vacuum distillation with intermediate drying over calcined potassium carbonate and molecular sieves. The salts used as supporting electrolytes were twice recrystallized (Et_4NBr, from MeCN and Et_4NBF_4, from EtOH) and dried in a vacuum drying chamber for 2 days at 100 °C. The alcohols were refluxed for 5 h over freshly prepared barium oxide and then distilled. Benzene and ether were dried by distillation over Na; chloroform was dried by refluxing over P_2O_5 with subsequent distillation.

The $NiBr_2bpy$ and $Ni(BF_4)_2bpy_3$ complexes were prepared from the corresponding nickel salt and the required amount of bpy in EtOH with stirring for 5 h. The precipitates formed were filtered off and dried in a vacuum chamber at 30 °C for 24 h. The organic halides (RX) used were chemically pure grade commercial reagents, which were purified by distillation until constant physical parameters were attained. The $(BuO)_3PO$ used as the label was purified by heating with metallic Na for 4 h at 100 °C followed by three vacuum distillations.

Processing of the results of voltammetric studies. The error of the peak potential measurements was ≤10 mV. The number of electrons transferred from an electrode to the nickel complex was determined by comparing the peak currents of the compound under study with the current of the first diffusion peak of benzophenone reduction (1e) under similar conditions.

The apparent rate constants (k_{app}) for catalyst regeneration were calculated by the Saveant method[2] using the approximating equation that relates the I_p^k/I_p^d ratio to k_{app} (I_p^k and I_p^d are the catalytic (kinetic) and diffusion currents, respectively).

The rate constants (k_1) for the oxidative addition of organic halides to σ-organonickel complex (mediator) were calculated by a previously described procedure[3] using the calibrating curves for different excess factors C_S^0/C_A^0 (C_S^0 is the substrate bulk concentration, C_A^0 is the mediator concentration) and the plot for the I_p^k/I_p^d ratio *vs.* $\log\chi k$, where χk is the kinetic parameter equal to $k_1 C_A^0 RT/(FV)$.

Electrochemical reduction of $NiBr_2bpy$ in the presence of alkyl iodides. The working solution (30 mL) was prepared by dissolving $NiBr_2bpy$ ($18.75 \cdot 10^{-2}$ g, $5 \cdot 10^{-4}$ mol), RI ($5 \cdot 10^{-3}$ mol; 0.5 mL of Pr^iI or 0.65 mL of Am^iI), and Et_4NBF_4 (1.085 g, $5 \cdot 10^{-3}$ mol) in DMF. Electrolyses were carried out in both divided and undivided electrochemical cells. During electrolysis, 0.27 A h^{-1} of electricity was passed at a controlled potential (−1.55 V). The reaction mixture was stirred under a continuous argon stream and analyzed by GLC when the electrolysis had been completed.

Electrochemical reduction of $NiBr_2bpy$ in the presence of aryl bromides. In the case of preparative reduction, a 30-mL working solutions was prepared by dissolving $NiBr_2bpy$ (0.1875 g, $5 \cdot 10^{-4}$ mol), Et_4NBr (1.05 g, $5 \cdot 10^{-3}$ mol), and RBr ($1 \cdot 10^{-3}$ mol; 0.1 mL of PhBr or 0.12 mL of 2-BrTol) in DMF. The complexes $Tol_2NiBrbpy$, $MesNiBrbpy$, and Mes_2Nibpy were prepared using 2-BrTol (0.12 mL, $1 \cdot 10^{-3}$ mol), MesBr (0.075 mL, $5 \cdot 10^{-4}$ mol), or MesBr (0.15 mL, $1 \cdot 10^{-3}$ mol), respectively. Electrolysis was carried out in the potentiostatic mode at a working electrode potential of −1.52 V *vs.* Ag/0.01 *M* $AgNO_3$ in MeCN. Electricity (27 mA h^{-1}) was passed through the electrolyte. The amounts of electricity passed for the preparation of $Tol_2NiBrbpy$, $MesNiBrbpy$, and Mes_2Nibpy were 40.5, 27, and 54 mA h^{-1}, respectively. After completion of electrolysis, the solvent was distilled off, and the products were extracted from the residue into ether. Then the ether was evaporated and the products were dried in a vacuum chamber at 30 °C.

(2,2′-Bipyridine)bromobis(2-tolyl)nickel, m.p. 145 °C (decomp.). Found (%): C, 60.34; H, 5.23; Br, 16.58; N, 6.03; Ni, 12.37. $C_{24}H_{22}NiN_2Br$. Calculated (%): C, 60.38; H, 4.61; Br, 16.77; N, 5.87; Ni, 12.37. ^{1}H NMR, δ: 8.56—8.57 (m, 2 H); 8.33—8.37 (d, 2 H); 7.79—7.82, 7.28—7.31 (both m, each 2 H); 7.10—7.14 (m, 6 H, C_6H_4); 6.92 (m, 2 H, C_6H_4); 1.91 (s, 6 H, Me).

(2,2′-Bipyridine)bromo(mesityl)nickel(II), m.p. 149 °C (decomp.). Found (%): C, 55.03; H, 4.60; Br, 18.90; N, 6.03; Ni, 14.16. $C_{19}H_{19}NiN_2Br$. Calculated (%): C, 55.14; H, 4.59; Br, 19.31; N, 6.77; Ni, 14.18. ^{1}H NMR, δ: 8.56—8.57 (m, 2 H); 8.33—8.37 (d, 2 H); 7.79—7.82, 7.28—7.31 (both m, each 2 H); 6.45 (m, 2 H, C_6H_2); 2.59 (s, 6 H, Me); 2.17 (s, 3 H, Me).

(2,2′-Bipyridine)bis(mesityl)nickel, m.p. 215 °C (decomp.). Found (%): C, 74.08; H, 6.83; N, 6.28; Ni, 12.37. $C_{28}H_{30}NiN_2$. Calculated (%): C, 74.19; H, 6.62; N, 6.18; Ni, 12.96. ^{1}H NMR, δ: 8.56—8.57 (m, 2 H); 8.33—8.37 (d, 2 H); 7.79—7.82, 7.28—7.31 (both m, each 2 H); 6.45 (m, 4 H, C_6H_2); 2.59 (s, 12 H, Me); 2.17 (s, 6 H, Me).

Results and Discussion

Reduction of aliphatic halides by nickel(0) bpy complexes. When RI (R = Pr^i, Am^i) is added to a solution of $Ni^{II}bpy_n$ (n = 1 or 3), the reduction current at the first-peak potential (Ni^{II}/Ni^0) substantially increases, while the anodic component disappears (Fig. 1).

When the $NiBr_2bpy$ is used as the initial complex, a new peak (Red_4) appears in the presence of RI. The peak occurs at more cathodic potentials (Table 1) and corresponds apparently to the reduction of $RNi^{II}Ibpy_n$

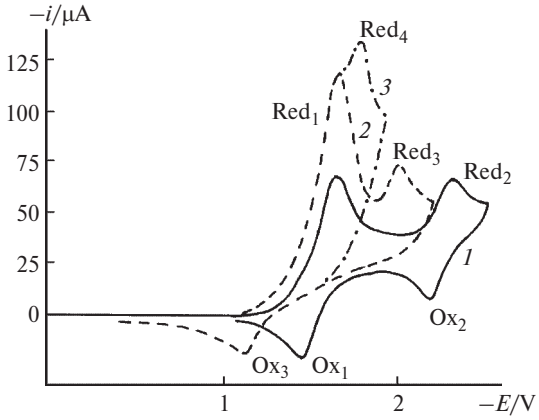

Fig. 1. CV curves for $Ni^{II}bpy$ (0.01 mol L^{-1}) in the absence (*1*) and in the presence (*2*, *3*) of Pr^iI in a concentration of 0.01 (*2*) and 0.1 mol L^{-1} (*3*).

Table 1. Peak potentials (E/V) in the CV curves of nickel complexes with 2,2′-bipyridine in the presence of aliphatic iodides (RI)[a]

Complex	RI[b]	$-E_{RI}$	Peak potentials ($-E_p$)						
			Red_1	Red_2	Red_3	Red_4	Ox_1	Ox_2	Ox_3
$Ni^{II}bpy_3$	Pr^iI	1.95	1.62	2.32	1.95	—	1.49	2.22	1.16
	Am^iI	2.09	1.62	2.32	2.09	—	1.49	2.22	0.87
$Ni^{II}bpy$	Pr^iI	1.95	1.55	2.23	1.95	1.65	1.38	2.12	1.16
	Am^iI	2.09	1.55	2.23	2.09	1.68	1.38	2.12	0.87

[a] Experimental conditions: DMF, 0.1 *M* Et_4NBF_4, GC, *vs.* Ag/0.01 *M* $AgNO_3$ in MeCN.
[b] The concentration of RI was $1 \cdot 10^{-2}$ mol L^{-1}.

(n = 1, 2), which has formed in the reaction of RI with the Ni^0 complex generated at the Red_1 potentials. The σ-alkylnickel complexes $AlkNi^{II}XL_2$ are known[4,5] to be thermodynamically unstable; they decompose with regeneration of the initial catalyst. However, the rate of this reaction is relatively low because the above-noted peak of $RNi^{II}XL_2$ reduction ($E_p^{Red_4}$) is still detectable. Therefore, it is assumed that this complex can be reduced competitively at the E^{Red_1} potentials under the action of Ni^0bpy_n (n = 1, 2). If we assume that the intermediate RNi^nXL_2 complex participates in three competing reactions and that for different R and X, the process steps are the same, only the rates being different, the following scheme of catalyst regeneration with RX can be proposed as the most probable (Scheme 1).

Scheme 1

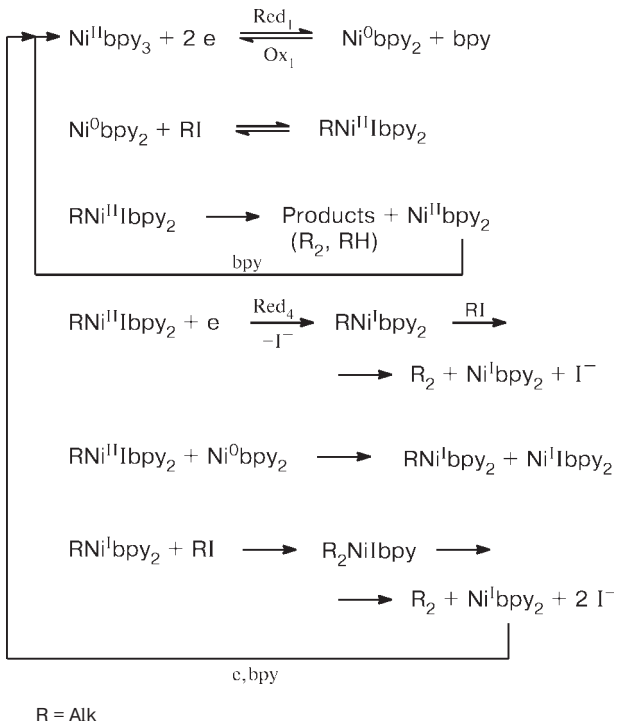

Curve *1* (see Fig. 1) confirms the reversibility of the Ni^{II}/Ni^0 redox pair; the potential difference between the anodic and cathodic peaks (130 mV) is exceeded because the bulk resistance of the solution is not counterbalanced. The GLC analysis of the reaction mixture obtained by exhaustive electrolysis of a mixture of $NiBr_2bpy$ with Pr^iI (1 : 10) at $E = -1.52$ V showed the formation of 2,3-dimethylbutane $(Pr^i)_2$ as the major product.

The catalytic efficiency of the nickel(0) complex whose Ni^{II} precursor contains one bpy ligand in the coordination sphere is higher than the efficiency of the catalyst formed from the nickel complex with three bpy ligands (Table 2). This fact is indicative of the substantial influence of the complex dissociation—association steps on the rate of the whole process. The considerable current growth observed at the reduction potentials of $Ni^{II}bpy_n$ complexes (n = 1, 3) in the presence of RI and the simultaneous disappearance of the anodic component of the Red_1 wave allows one to calculate the effective rate constant for catalyst regeneration k_{app} (see Table 2) using the Saveant method.[2]

The dependence of the number of electrons (n_e) transferred at the potentials of the first reduction step (Red_1), which implies Ni^{II} to Ni^0 transition, on the square root of the concentration of the [RI] substrate added (Fig. 2) is linear for a relatively small excess of RI, *i.e.*, the overall process obeys the first order kinetics with respect to the substrate and the reaction rate is determined by the oxidative addition step (see Scheme 1). For high sub-

Table 2. Effective rate constants for catalyst regeneration (k_{app}) ($1 \cdot 10^{-2}$ mol L^{-1}) in the presence of RI at the potential $E_p^{Red_1}$

Complex	RI	$[RI] \cdot 10^2$ /mol L^{-1}	I_p^k/I_p^{d*}	$k_{app} \cdot 10^{-1}$ /L mol^{-1} s^{-1}
$Ni^{II}bpy_3$	Pr^iI	10.8	2.09	2.8
	Am^iI	11.1	2.09	3.0
$Ni^{II}bpy$	Pr^iI	10.8	2.65	5.0
	Am^iI	9.2	2.40	4.9

* Ratio of the catalytic (kinetic) and diffusion currents.

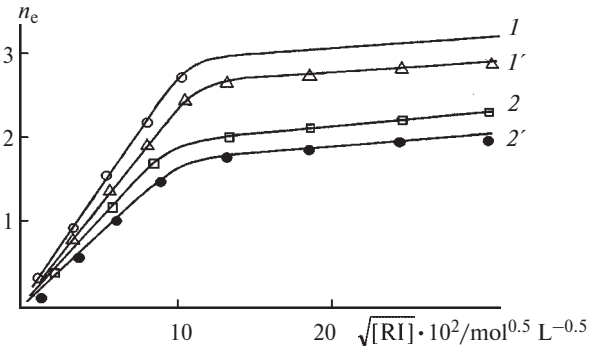

Fig. 2. Number of electrons (n_e) transferred at potentials of the first step of reduction (Red_1) of $Ni^{II}bpy$ (*1*, *1′*) and $Ni^{II}bpy_3$ (*2*, *2′*) (0.01 mol L^{-1}) in the presence of Pr^iI (*1*, *2*) and Am^iI (*1′*, *2′*) *vs.* [RI].

strate concentrations, the Red_1 peak current does not depend on the concentration. This implies saturation at which the reaction follows a zero order with respect to the substrate and a subsequent reaction, for example reductive elimination, is the rate-determining step.

The addition of aliphatic bromides does not induce catalytic increase in the current at the first-peak Red_1 potentials, and the process reversibility is not deteriorated (Fig. 3). Apparently, in these cases, the key steps responsible for the catalyst regeneration are too slow; this hampers detection of these steps under CV conditions.

The experiments show that the primary products of the oxidative addition of $AlkNiXbpy_n$ (n = 1, 2) are relatively unstable under the experimental conditions, which precludes using them as model compounds to study cross-coupling reactions.

The reaction of aromatic halides with electrochemically generated nickel(0) bpy complexes. As model aryl halides (ArX), we chose PhBr, PhI, 2-BrTol, and MesBr. By using this series of substrates, one can model and compare the reaction pathways involving intermediates

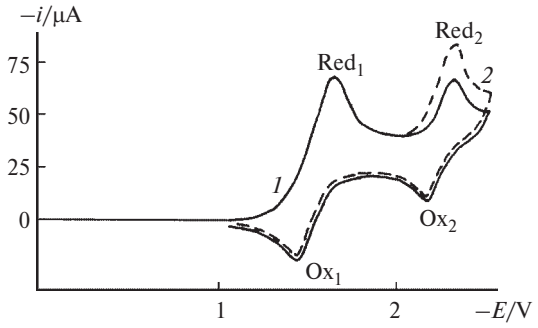

Fig. 3. CV curves for $Ni(BF_4)bpy_3$ (0.01 mol L^{-1}) in the absence (*1*) and in the presence of BuBr (0.01 mol L^{-1}) (*2*).

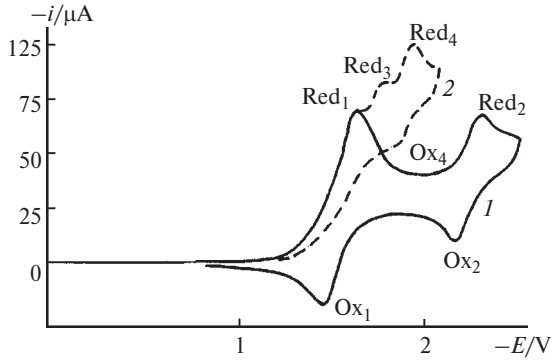

Fig. 4. CV curves for $Ni(BF_4)_2bpy_3$ (0.01 mol L^{-1}) in the absence (*1*) and in the presence of PhI (0.02 mol L^{-1}) (*2*).

differing in stability, due to the presence of the Me group in the *ortho*-position of the benzene ring.

In the CV curves recorded for the $Ni(BF_4)_2bpy_3$ complex in the presence of PhI, the Ox_1 anodic peak disappears, while two new cathodic peaks (Red_3 and Red_4) appear at more negative potentials (Fig. 4), the latter of the two being reversible (has an anodic component, Ox_4). The total current of the Red_3 and Red_4 peaks is directly proportional to [PhI] (Fig. 5), which attests to a catalytic nature of the process that takes place at the potentials of these peaks.[2] In the case of $NiBr_2bpy$, which is coordinatively unsaturated with respect to bpy, the increase in the current of the Red_3 and Red_4 peaks upon the addition of the corresponding amounts of PhI is more pronounced. Thus, the regeneration rates of the Ni^0bpy catalyst and of the catalytic cycle intermediates are much higher, indicating that the dehalogenation by the $Ni^{II}bpy$ complex is more efficient than that by the $Ni^{II}bpy_3$ complex (see Fig. 5).

When ArBr is added to the $Ni^{II}bpy_3$ complex, the Red_1 peak (reduction of Ni^{II} to Ni^0) remains unchanged and retain its reversibility, and no other peaks indicating reduction of the oxidative addition products at more cathodic potentials can be detected (Fig. 6, *a*). Thus, the

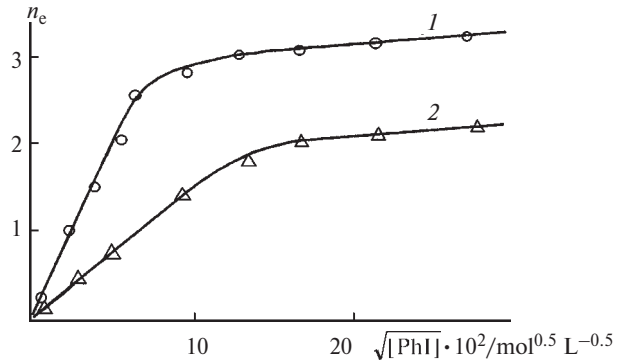

Fig. 5. Total current of the Red_3 and Red_4 reduction peaks of $Ni^{II}bpy$ (*1*) and $Ni^{II}bpy_3$ (*2*) *vs.* [PhI].

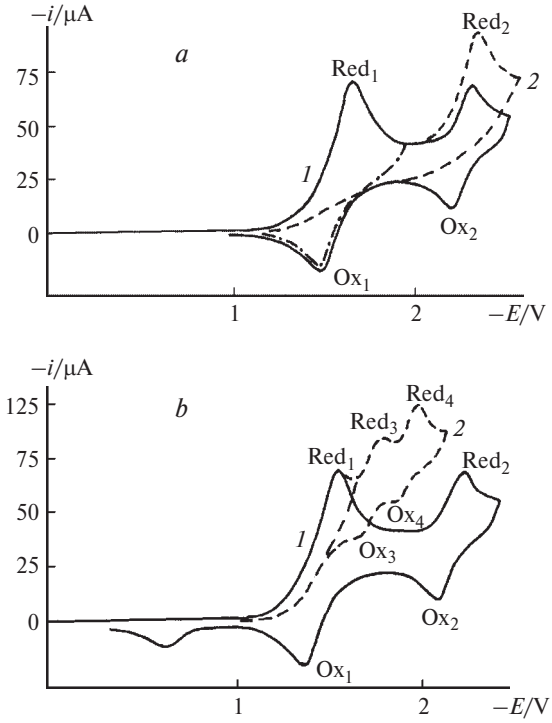

Fig. 6. CV curves for $Ni(BF_4)_2bpy_3$ (*a*) and $NiBr_2bpy$ (*b*) (0.01 mol L^{-1}) in the absence (*1*) and in the presence of PhBr (0.01 mol L^{-1}) (*2*).

Ni^0bpy_n complex (n = 1, 2) obtained from $Ni^{II}bpy_3$ does not exhibit catalytic activity under CV conditions. A catalytic gain in the current can be observed only at the potential of the second peak Red_2 (see Fig. 6, *a*), corresponding to the formation of $Ni^0bpy_2^{\cdot -}$ (Scheme 2).

The effective rate constants for regeneration of the catalyst of this process are presented in Table 3. The highest k_{app} is observed in the case of PhBr; the presence of *ortho*-substituents decreases this value.

The $NiBr_2bpy$ complex, coordinatively unsaturated with respect to bpy, proved to be much more active in electrochemical dehalogenation. When $NiBr_2bpy$ is reduced in the presence of ArBr, the reversibility of the first Red_1 peak disappears (Fig. 6, *b*). This implies a rather high rate of the oxidative addition step, decreasing in the series of substrates PhBr > 2-BrTol > MesBr.

Table 3. Effective rate constants (k_{app}) for regeneration of the $Ni^{II}bpy_3$ catalyst ($1 \cdot 10^{-2}$ mol L^{-1}) in the presence of ArBr at the potential $E_p^{Red_2}$

ArBr	[ArBr]·10^2 /mol L^{-1}	I_p^k/I_p^{d*}	$k_{app} \cdot 10^{-1}$ /L mol^{-1} s^{-1}
PhBr	12.0	3.24	4.0
2-BrTol	12.0	2.22	1.6
MesBr	11.7	1.38	0.6

* Ratio of the catalytic (kinetic) and diffusion currents.

Scheme 2

$$Ni^{II}bpy_3 + 2\,e \underset{Ox_1}{\overset{Red_1}{\rightleftharpoons}} Ni^0bpy_2 + bpy$$

$$Ni^0bpy_2 + e \underset{Ox_2}{\overset{Red_2}{\rightleftharpoons}} [Ni^0bpy_2]^{\cdot -}$$

$$[Ni^0bpy_2]^{\cdot -} + ArBr \xrightarrow{k} Ni^0bpy_2 + 0.5\,Ar_2 + Br^-$$

$$Ni^0bpy + ArBr \longrightarrow ArNi^{II}Brbpy.$$

The published data[6] suggest that the Red_3 and Red_4 peaks (Table 4) correspond to the reduction of the oxidative addition products, σ-aryl nickel complexes; however, the structure of these complexes is unknown. We attempted to elucidate their nature by using preparative electrolysis and CV methods.

After passing 2 F of electricity (per Ni atom) at the potential E^{Red_1} through an electrolyte containing $NiBr_2bpy$ and PhBr (1 : 2) in DMF in an undivided cell with a Mg

Table 4. Peak potentials (E_p) in the CV curves for $Ni^{II}bpy_3$ and $Ni^{II}bpy$in the presence of ArX

Complex	ArX	$-E_p$/V							
		Red_1	Red_2	Red_3	Red_4	Ox_1	Ox_2	Ox_3	Ox_4
$Ni^{II}bpy_3$	PhI	1.62	2.32	1.76	1.98	1.49	2.22	—	1.77
	PhBr	1.62	2.32	—	—	1.49	2.22	—	—
	2-BrTol	1.62	2.32	—	—	1.49	2.22	—	—
	MesBr	1.62	2.32	—	—	1.49	2.22	—	—
$Ni^{II}bpy$	PhI	1.55	2.28	1.74	1.95	1.38	2.16	—	—
	PhBr	1.55	2.28	1.76	1.96	1.38	2.16	1.63	1.82
	2-BrTol	1.55	2.28	1.77	1.96	1.38	2.16	1.65	1.83
	MesBr	1.55	2.28	1.80	2.01	1.38	2.16	1.77	1.90

Note. Experimental conditions: DMF, 0.1 *M* Et_4NBF_4, GC, *vs.* Ag/0.01 *M* $AgNO_3$ in MeCN.

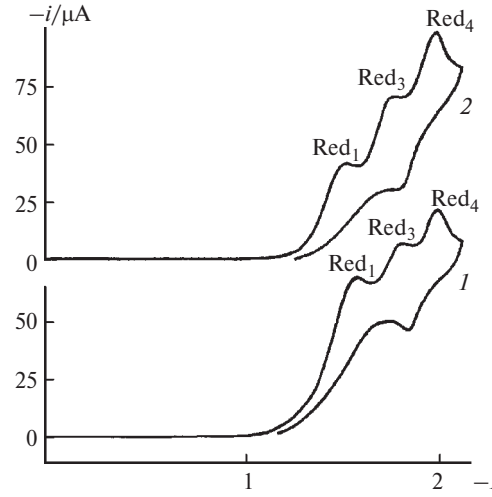

Fig. 7. CV curves for $NiBr_2bpy$ (0.01 mol L^{-1}) in the presence of PhBr (0.02 mol L^{-1}) before electrolysis (*1*) and after passing of 2 *F* of electricity (*2*).

anode, the CV curve exhibits the same peaks, Red_1, Red_3, and Red_4. The current of the Red_1 peak somewhat decreases, while the height of the peaks at $E_p^{Red_3}$ and $E_p^{Red_4}$ increases with respect to the values observed prior to electrolysis, so that the three peaks have identical heights (Fig. 7). GLC analysis of the reaction mixture after electrolysis showed the presence of biphenyl. Thus, the product of oxidative addition of PhNiBrbpy is insufficiently stable under the given conditions and the catalyst is generated at the potential E^{Red_1}.

To identify the limiting steps of the process, we studied the dependences of the heights of the Red_3 and Red_4 cathodic peaks on the ArBr concentration (Fig. 8). The total current of the peaks observed at $E_p^{Red_3}$ and $E_p^{Red_4}$ increases in proportion to [PhBr] and does not depend on the concentration of the complex. These dependences are typical of catalytic processes involving regeneration of the active form of the catalyst;[2] this prompts the following scheme for the given process (Scheme 3).

Scheme 3

$$PhNi^{II}Brbpy + e \rightleftharpoons PhNi^{I}bpy + Br^- \quad (1)$$

$$PhNi^{I}Brbpy + PhBr \longrightarrow Ph_2NiBrbpy + Br^- \quad (2)$$

$$Ph_2NiBrbpy \longrightarrow Ph_2 + NiBrbpy \quad (3)$$

$$Ni^{I}bpy + e \rightleftharpoons Ni^{0}bpy \quad (4)$$

$$Ni^{0}bpy + PhBr \longrightarrow PhNi^{II}Brbpy \quad (5)$$

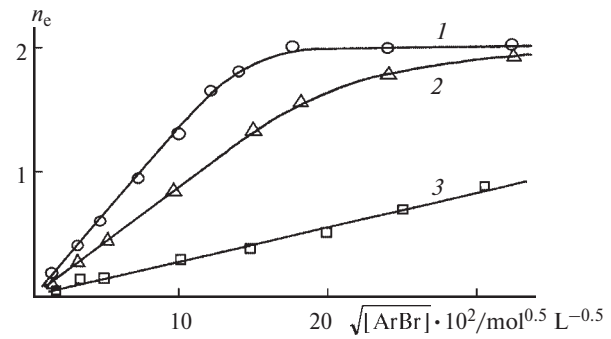

Fig. 8. Total number of electrons (n_e) transferred at the potentials of the Red_3 and Red_4 cathodic peaks of $Ni^{II}bpy$ и $Ni^{II}bpy_3$ in the presence of PhBr (*1*), 2-BrTol (*2*), and MesBr (*3*) *vs.* [ArBr].

When the PhBr concentration is high, the number of electrons corresponding to the Red_3 and Red_4 steps tends to a definite limit and no longer depends on the PhBr concentration. This proves that the overall rate of the process described by this scheme (see Scheme 3) is now controlled by a step having a zero order with respect to the substrate and the first order with respect to nickel. Indeed, the reduction of $Ni^{I}Brbpy$ is highly exoergic at potentials of the Red_3 peak because the reduction potential of Ni^{II} to Ni^0 is much more positive. Step (5) is rather fast compared to other steps,[7–9] so that it cannot be responsible for the kinetic control of the whole sequence (see Scheme 3). Thus, for low PhBr concentrations, oxidative addition is the limiting step (see Scheme 3, reaction (2)) and the reaction has the first orders with respect to PhBr and nickel.

When the PhBr concentration is high, this step becomes rather fast, so that the process is limited by reductive elimination (see Scheme 3, reaction (3)). The proposed sequence (see Scheme 3) is in qualitative agreement with the concentration dependences of the reduction currents at $E_p^{Red_3}$ and $E_p^{Red_4}$.

Thus, the stability of σ-phenyl nickel complexes is low, so they cannot be used to model more complex cross-coupling reactions involving RX. In this case, the homocoupling product, *viz.*, biphenyl, is formed in each step, *viz.*, Red_1, Red_3, and Red_4.

The stability of the transition metal aryl σ-complexes having a Me group in the *ortho*-position of the aromatic nucleus is caused by steric factors, which hamper the rotation about the Ar—metal σ-bond and the axial attack of the reagents on the nickel atom.[10] Let us consider ER of the $Ni^{II}bpyBr_2$ complex in the presence of 2-BrTol (Fig. 9).

After electrolysis of the working solution containing $Ni^{II}bpyBr_2$ and 2-BrTol (1 : 2) at the potential $E_p^{Red_1}$, the Red_1 peak disappears from the CV curve, whereas the Red_3 and Red_4 peaks whose total current corresponds to the participation of two electrons are retained (see

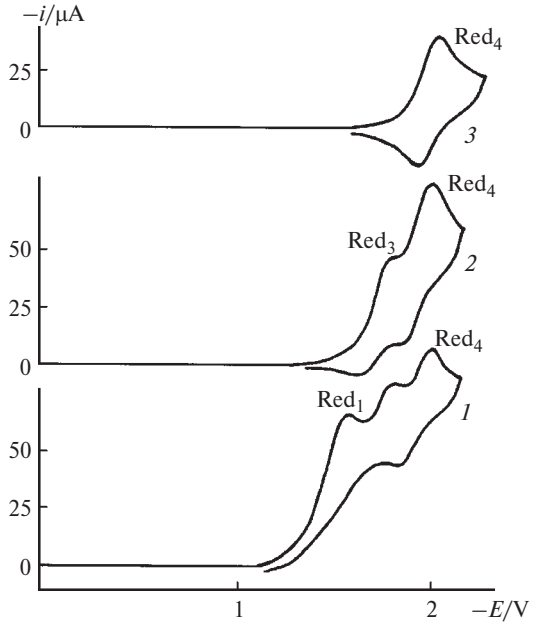

Fig. 9. CV curves for $NiBr_2bpy$ (0.01 mol L^{-1}) in the presence of 2-BrTol (0.01 mol L^{-1}) before electrolysis (*1*) and after passing of 2 *F* (*2*) and 3 *F* (*3*) of electricity per nickel complex molecule.

Fig. 9). Both peaks are reversible but for Red_4, the anodic component is undoubtedly more pronounced. The solution acquires a red color corresponding to the TolNiBrbpy σ-complex, which is formed, in our opinion, upon oxidative addition (reaction (7)).

$$NiBr_2bpy + 2\,e \underset{Ox_1}{\overset{Red_1}{\rightleftharpoons}} Ni^0bpy + 2\,Br^-, \qquad (6)$$

$$Ni^0bpy + 2\text{-BrTol} \longrightarrow TolNiBrbpy. \qquad (7)$$

Upon the addition of 2-BrTol to a solution of TolNiBrbpy, the height of the Red_3 peak does not change, while the current of the Red_4 peak is directly proportional to [2-BrTol]. However, the Tol_2 dimer is not formed in the solution, *i.e.*, the addition of TolNiBrbpy to TolBr does not take place. Thus, the σ-complex prepared from 2-BrTol by reaction (7) is rather stable in solution and can be used to study the mechanism of RX cross-coupling or other reactions involving these substrates.

The CV curves for the $NiBr_2bpy$ complex in the presence of increasing amounts of 2-BrTol display a slight gain in the current at the potentials of the Red_3 and Red_4 peaks. At higher concentrations, the total current of the Red_3 and Red_4 peaks tends to a limit corresponding to the addition of approximately two electrons per nickel complex.

After electrolysis of a solution of TolNiBrbpy at $E_p^{Red_3} = 1.77$ V (1 *F* mol^{-1} per Ni atom), the CV curve of the solution exhibits one reversible Red_4 peak ($E_p^{Red_4} = -1.96$ V). The solution has an intense vinous-lilac color. The new nickel complex was isolated and characterized by spectroscopy and elemental analysis as $Tol_2NiBrbpy$. The CV curve of this compound exhibits one reversible single-electron reduction peak with $E_p^{Red_4} = -1.96$ V and one single-electron oxidation peak (Br^-) at a potential of +0.12 V (Fig. 10). The complex slowly decomposes in air, and after 6—7 h, the electrolyte solution develops a green color, typical of $NiBr_2bpy$ (this was confirmed by CV), and the content of ditolyl in the solution increases 20-fold. The following scheme can be proposed for the formation of σ-ditolyl nickel complex during electrolysis at $E_p^{Red_3}$:

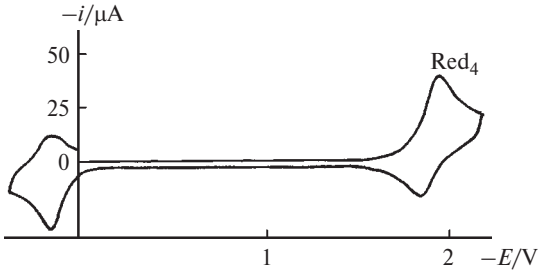

Fig. 10. CV curve for $Tol_2NiBrbpy$ (0.01 mol L^{-1}).

$$TolNi^{II}Brbpy + e \overset{E_p^{Red_3}}{\rightleftharpoons} TolNi^{I}bpy + Br^-,$$

$$TolNi^{I}bpy + TolBr \longrightarrow Tol_2NiBrbpy.$$

Under CV conditions, this complex is reversibly reduced (see Fig. 10):

$$Tol_2NiBrbpy + e \overset{E_p^{Red_4}}{\rightleftharpoons} [Tol_2NiBrbpy]^{\bullet -}.$$

By analogy with the data published previously,[11] one can suggest that in the radical anion formed, the electron is concentrated on the ligand. The radical anion would apparently reduce 2-BrTol, as an outer-sphere electron transporter, to give toluene, whose presence in the reaction mixture was confirmed by GLC analysis. Slow decomposition of $[Tol_2NiBrbpy]^{\bullet -}$ in the solution to give ditolyl might be a competing process.

The fact that the ER products formed at this step contain no $Nibpy^{2+}$ derivatives was confirmed by CV curves, specifically, the Red_4 peak gradually disappears and the cathodic region contains no peaks up to reduction of the supporting electrolyte.

The use of MesBr instead of 2-BrTol results in the more stable σ-complex, $MesNi^{II}Brbpy$, which can be used subsequently as a model compound to study cross-coupling of RX in the absence of the primary substrate (2-TolBr or MesBr).

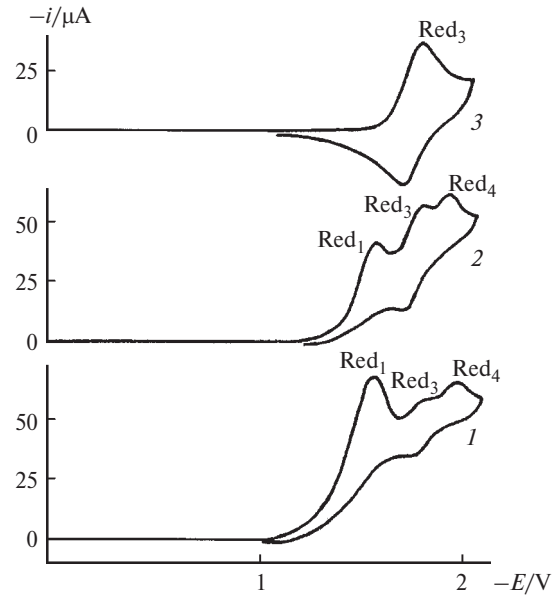

Fig. 11. CV curves for $NiBr_2bpy$ (0.01 mol L^{-1}) in the presence of MesBr (0.01 mol L^{-1}) before electrolysis (*1*) and after passing of 1 *F* (*2*) and 2 *F* (*3*) of electricity.

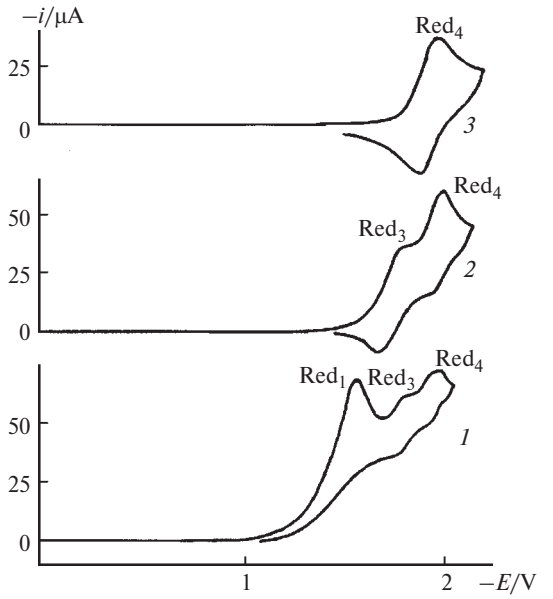

Fig. 12. CV curves for $NiBr_2bpy$ (0.01 mol L^{-1}) in the presence of MesBr (0.02 mol L^{-1}) before electrolysis (*1*) and after passing of 2 *F* (*2*) and 4 *F* (*3*) of electricity.

Now we consider the reduction of $NiBr_2bpy$ in the presence of MesBr. In the electrolysis of a solution containing $Ni^{II}bpy$ ($1 \cdot 10^{-2}$ mol L^{-1}) and MesBr ($1 \cdot 10^{-2}$ mol L^{-1}) at $E_p^{Red_1}$ (−1.55 V), the CV curve recorded after passing 2 *F* of electricity exhibits (Fig. 11, curve *3*) one reversible single-electron Red_3 peak, which corresponds most likely to the reduction of the σ-complex (Scheme 4).

Scheme 4

$$Ni^{II}bpy + 2\,e \xrightarrow[2\,F]{-1.55\ V} Ni^{0}bpy$$

$$Ni^{0}bpy + MesBr \longrightarrow MesNiBrbpy$$

$$MesNiBrbpy + e \overset{E_p^{Red_3}}{\rightleftharpoons} [MesNiBrbpy]^{\cdot -} \rightleftharpoons$$

$$\rightleftharpoons MesNi^{I}bpy + Br^{-}$$

When the MesNiBrbpy complex is reduced in the presence of some excess of bpy (this is necessary to suppress dimerization of the $MesNi^{I}bpy$ species in the absence of RX), the formation of the paramagnetic $MesNi^{I}bpy$ complex was detected by ESR, *i.e.*, reversible nickel-centered electron transfer takes place.

The presence of two Me groups in the *ortho*-position retards not only the reductive elimination but also the oxidative addition involving nickel σ-mesityl complexes. Let us consider the reduction of a solution of $Ni^{II}bpy$ and MesBr (1 : 2) in DMF in a divided cell. After passing 2 *F* of electricity at $E_p^{Red_1} = -1.55$ V, the CV curve has two reversible single-electron peaks, Red_3 and Red_4, which resembles the situation with 2-BrTol. The four-electron reduction of $Ni^{II}bpy$ in the presence of MesBr (1 : 2) results in the selective formation of the nickel dimesityl complex Mes_2Nibpy, which is reduced at the potential E^{Red_4} (Fig. 12, curve *3*). This complex was isolated from the solution and characterized by spectroscopy and elemental analysis. Thus, the rate constant for the oxidative addition (k_1)

$$ArNi^{I}bpy + ArBr \xrightarrow{k_1} Ar_2NiBrbpy$$

is lowerfor MesBr than that for 2-BrTol. The product of reduction of $Ar_2NiBrbpy$ at the potential E^{Red_4} is more stable in the case of MesBr; this product is the diaryl nickel complex, Mes_2Nibpy, formed by the reaction

$$Mes_2NiBrbpy + e \overset{Red_4}{\rightleftharpoons} Mes_2Nibpy + Br^{-}.$$

This work was supported by the Russian Foundation for Basic Research (Projects No. 01-03-33210-a and No. 01-15-99353-m) and by a Joint Program of the CRDF and the RF Ministry of Education "Research and Educational Center of KSU," REC 007, and the Integrated Program of the Russian Academy of Sciences "New Principles and Methods for the Design and Targeted Synthesis of Substances with Specified Properties," and by the INTAS (Grant 00-0018).

References

1. H. Lemkuhl, *Synthesis*, 1973, 377.
2. C. P. Andrieux and J. M. Saveant, in *Investigations of Rates and Mechanisms of Reactions*, Wiley, New York, 1986, 305.
3. S. U. Pedersen and B. Svensmark, *Acta Chem. Scand.*, 1986, **9**, 607.
4. P. W. Jolly and G. Wilke, *The Organic Chemistry of Nickel. Part 2. Organic Synthesis*, Academic Press, New York, 1975, 416 pp.
5. G. Shiavon, G. Bontempelli, and B. Corain, *J. Chem. Soc., Dalton Trans.*, 1981, **5**, 1074.
6. M. Durandetti, M. Devaud, and J. Perichon, *New J. Chem.*, 1996, **20**, 659.
7. C. Amatore and A. Jutand, *Organometallics*, 1988, **7**, 2203.
8. C. Amatore, A. Jutand, and L. Mottier, *J. Electroanal. Chem.*, 1991, **306**, 125.
9. C. Amatore, A. Jutand, and L. Mottier, *J. Electroanal. Chem.*, 1991, **306**, 141.
10. J. Chatt and B. L. Shaw, *J. Chem. Soc.*, 1960, **4**, 1718.
11. W. Kaim, *Coord. Chem. Rev.*, 1987, **76**, 187.

Received July 20, 2001;
in revised form December 26, 2001